

Compressible Magnetohydrodynamic Turbulence in the Earth's Magnetosheath: Estimation of the Energy Cascade Rate Using *in situ* Spacecraft Data

L. Z. Hadid*

Swedish Institute of Space Physics, SE 751 21, Uppsala, Sweden
and LPP, CNRS, Ecole Polytechnique, Université Paris-Sud, Observatoire de Paris, Université Paris-Saclay, Sorbonne Université, PSL Research University, 91128 Palaiseau, France

F. Sahraoui

LPP, CNRS, Ecole Polytechnique, Université Paris-Sud, Observatoire de Paris, Université Paris-Saclay, Sorbonne Université, PSL Research University, 91128 Palaiseau, France

S. Galtier

LPP, CNRS, Ecole Polytechnique, Université Paris-Sud, Observatoire de Paris, Université Paris-Saclay, Sorbonne Université, PSL Research University, 91128 Palaiseau, France

S. Y. Huang

School of Electronic Information, Wuhan University, Wuhan 430072, China



(Received 26 May 2017; revised manuscript received 18 October 2017; published 29 January 2018)

The first estimation of the energy cascade rate $|e_C|$ of magnetosheath turbulence is obtained using the *Cluster* and *THEMIS* spacecraft data and an exact law of compressible isothermal magnetohydrodynamics turbulence. The mean value of $|e_C|$ is found to be close to $10^{-13} \text{ J m}^{-3} \text{ s}^{-1}$, at least 2 orders of magnitude larger than its value in the solar wind ($\sim 10^{-16} \text{ J m}^{-3} \text{ s}^{-1}$ in the fast wind). Two types of turbulence are evidenced and shown to be dominated either by incompressible Alfvénic or compressible magnetosoniclike fluctuations. Density fluctuations are shown to amplify the cascade rate and its spatial anisotropy in comparison with incompressible Alfvénic turbulence. Furthermore, for compressible magnetosonic fluctuations, large cascade rates are found to lie mostly near the linear kinetic instability of the mirror mode. New empirical power-laws relating $|e_C|$ to the turbulent Mach number and to the internal energy are evidenced. These new findings have potential applications in distant astrophysical plasmas that are not accessible to *in situ* measurements.

DOI: [10.1103/PhysRevLett.120.055102](https://doi.org/10.1103/PhysRevLett.120.055102)

Turbulence is a ubiquitous nonlinear phenomenon in hydrodynamic and plasma flows that dynamically transfers energy between different scales. In astrophysical plasmas, turbulence is thought to play a major role in various processes such as accretion disks, star formation, acceleration of cosmic rays, solar corona and solar wind heating, and energy transport in planetary magnetospheres [1–4]. Thanks to the availability of *in situ* measurements recorded on board various orbiting spacecraft, the solar wind and the Earth's magnetosheath (i.e., the region of the solar wind downstream of the bow shock) provide a unique laboratory for the observational studies of plasma turbulence. An important feature of magnetosheath turbulence is the high level of density fluctuations in it, which can reach $\sim 50\%$ – 100% [5–8] in comparison with $\sim 5\%$ – 20% in the solar wind [9,10]. This makes the magnetosheath a key region of the near-Earth space where significant progress can be made in understanding compressible plasma turbulence, which is poorly understood although it is thought to be

important in various astrophysical plasmas, such as supernovae remnants or the interstellar medium (ISM) [11–15].

In the solar wind, the magnetohydrodynamics (MHD) approximation has been successfully used to study turbulence cascade at scales larger than the ion inertial length (or Larmor radius) [16,17]. As in neutral fluid turbulence, an inertial range of MHD turbulence is generally evidenced by the observation of a power spectral density (PSD) exhibiting a power law over a wide range of scales. This power law is a manifestation of a turbulent cascade of energy from large scales, where the energy is injected, to the smaller ones where the energy is dissipated. The energy transfer over scales is assumed to occur at a constant rate, which is equal to the rate at which energy is injected and dissipated into the system. Therefore, this quantity carries a major importance in modeling the processes of particle acceleration and heating in plasmas since it provides an estimation of the amount of energy that is eventually handed to the plasma particles at the dissipation scales [18]. Within the

incompressible MHD turbulence theory, the energy cascade rate can be estimated using the so-called third-order law relating the longitudinal structure functions of the magnetic and the velocity fields, to the spatial scale l (Politano and Pouquet 1998, PP98 hereafter) [19]. The PP98 model has been used to estimate the cascade rate in the solar wind from the *ACE* and *ULYSSES* spacecraft data [20–26]. Those estimations were used to better understand the long-standing problem of the nonadiabatic heating of the solar wind observed at different heliospheric distances (~ 0.3 – 100 A.U. or astronomical units) by the *Helios* [27,28], *Pioneer*, and *Voyager* spacecraft [29–31]. To date, no such estimation of the cascade rate exists for magnetosheath turbulence. The main reason for that being the complex nature of magnetosheath turbulence and the importance of density fluctuations in it, which requires going beyond the PP98 model to include compressibility. Recently, an exact law of compressible isothermal MHD turbulence has been derived (Banerjee and Galtier 2013, hereafter BG13) [32]. It has been successfully used to improve our understanding of the role of density fluctuations in heating the fast and slow solar wind by showing, in particular, that, even if they are weak and represent only $\sim 5\%$ – 20% of the total fluctuations, they, nevertheless, can significantly enhance the turbulence cascade rate [10,33].

In the present Letter, we provide the first estimate of the energy cascade rate of compressible MHD turbulence in the Earth’s magnetosheath using the BG13 and *in situ* wave and plasma data. Furthermore, we investigate how density fluctuations amplify the energy cascade rate and how they affect its spatial anisotropy. The role of density fluctuations is highlighted by comparing the results obtained from the compressible BG13 and the incompressible PP98 exact laws. Under the assumptions of time stationarity, space homogeneity and isotropic turbulence, the PP98 exact law is given by

$$-\frac{4}{3}\varepsilon_I \ell = \left\langle \frac{(\delta \mathbf{z}^+)^2}{2} \delta z_\ell^- + \frac{(\delta \mathbf{z}^-)^2}{2} \delta z_\ell^+ \right\rangle \rho_0, \quad (1)$$

and the BG13 model is given by

$$\begin{aligned} -\frac{4}{3}\varepsilon_C \ell = & \left\langle \frac{1}{2} [\delta(\rho \mathbf{z}^-) \cdot \delta \mathbf{z}^-] \delta z_\ell^+ + \frac{1}{2} [\delta(\rho \mathbf{z}^+) \cdot \delta \mathbf{z}^+] \delta z_\ell^- \right\rangle \\ & + \langle 2\delta\rho\delta e\delta v_\ell \rangle + \left\langle 2\bar{\delta} \left[\left(1 + \frac{1}{\beta} \right) e + \frac{v_A^2}{2} \right] \delta(\rho_1 v_\ell) \right\rangle, \end{aligned} \quad (2)$$

where $\mathbf{z}^\pm = \mathbf{v} \pm \mathbf{v}_A$ represent the Elsässer variables, \mathbf{v} being the plasma flow velocity, $\mathbf{v}_A \equiv \mathbf{B}/\sqrt{\mu_0\rho}$ is the Alfvén speed, $\rho = \rho_0 + \rho_1$ is the local plasma density ($\rho_0 = \langle \rho \rangle$ and ρ_1 are the mean and fluctuating density), $\delta \mathbf{z}^\pm \equiv \mathbf{z}^\pm(\mathbf{x} + \ell) - \mathbf{z}^\pm(\mathbf{x})$ is the spatial increment of \mathbf{z}^\pm at a scale ℓ in the radial direction, $\langle \dots \rangle$ is the ensemble

average, $\bar{\delta}\psi \equiv [\psi(\mathbf{x} + \ell) + \psi(\mathbf{x})]/2$, $e = c_s^2 \ln(\rho/\rho_0)$ is the internal energy, with c_s the constant isothermal sound speed, and $\beta = 2c_s^2/v_A^2$ is the local ratio of the total thermal to magnetic pressure ($\beta = \beta_e + \beta_p$). Note that, in the PP98 model, ρ is replaced by ρ_0 in the definition of the Alfvén speed. Furthermore, the reduced form of BG13 used here assumes the statistical stationarity of the plasma β and the negligible contribution of the energy source terms with respect to flux terms [33]. It is worth noting that, contrary to incompressible MHD theory, the BG13 compressible model yields an energy cascade rate that is not related only to third-order moments of the different field increments, but rather involves more complex combinations of the turbulent fields. In particular, the last term in the rhs of Eq. (2) is written as a first order increment multiplied by an averaged quantity $\bar{\delta}\psi$. This term, that plays a leading order in the BG13 model [10,33], is likely to converge faster than the usual third-order terms when estimated from spacecraft observations or simulations data.

Results.—The data used here were measured by the *Cluster* and *THEMIS B/C* spacecraft [34,35]. Combining the data from the two missions was aimed at increasing the sample size of our study for a better statistical convergence. The magnetic field measurements of *Cluster* come from the flux gate magnetometer (FGM) [36], while the ion and electron plasma moments (density, velocity, and temperature) come from the Cluster Ion Spectrometer (CIS) experiment [37], and the Plasma Electron and Current experiment (PEACE) [38], respectively. Special attention has been paid to the reliability of the plasma data, in particular, the plasma density measurements, through cross checks between the PEACE, CIS, and the Waves of High Frequency and Sounder for Probing of Electron Density by Relaxation (WHISPER) experiments [39] on board *Cluster* (we selected only intervals when the instruments were consistent with each other). For *THEMIS* spacecraft, the magnetic field data and the plasma moments are measured, respectively, by the FGM [40] and the electrostatic analyzer [41]. In selecting our samples, we eliminated time intervals that contained significant disturbances or velocity shears and considered only time intervals that have a relatively stationary plasma β (as discussed above) [10].

A large statistical survey of PSD of δB in the magnetosheath using the *Cluster* data showed that only a small fraction (17%) had a scaling close to the Kolmogorov spectrum $f^{-5/3}$ at the MHD scales and were dominated either by incompressible Alfvénic or compressible magnetosonic fluctuations [42]. Those data sets correspond to a state of fully developed turbulence that is reached away from the bow shock toward the magnetosheath flanks. The remaining cases were found to have shallower spectra close to f^{-1} and were distributed essentially near the bow shock toward the nose of the magnetopause. Hadid *et al.* [43] showed that the f^{-1} spectra were populated by uncorrelated fluctuations. Here, since we are interested in estimating the

energy cascade rate, we focus only of the Kolmogorov-like cases that correspond to a fully developed turbulence where an inertial range can be evidenced. The final data selection resulted in 47 time intervals of equal duration 48 mn, which corresponds to a number of data points $N \sim 240$ in each interval with a 12 s time resolution ($N_{\text{tot}} \sim 2 \times 10^4$). The resulting samples were divided into two groups depending on the nature of the dominant turbulent fluctuations: incompressible Alfvénic-like and compressible magnetosoniclike ones. This was done using the magnetic compressibility $C_{\parallel} = \delta B_{\parallel}^2 / \delta B^2$ (i.e., the ratio between the PSDs of the parallel to the total magnetic fluctuations; parallel being along the mean background field \mathbf{B}_0) [43–46]. Figure 1 shows two examples of an Alfvénic-like event characterized by a nearly constant B , a subdominant δB_{\parallel} and weak density fluctuations, and a compressible case having large B and density fluctuations and a strong δB_{\parallel} .

For each of these groups, we computed the absolute values of the cascade rates $|\epsilon_C|$ and $|\epsilon_I|$ from the compressible BG13 and the incompressible PP98 models, respectively. To do so, temporal structure functions of the different turbulent fields involved in Eqs. (2) and (1) were constructed for different values of the time lag τ between 10 and 1000 s in order to probe into the scales of the inertial range (a statistical convergence test [47] is presented in the Supplemental Material [48]). In this Letter, we considered magnitude of the cascade rate rather than its signed value (assuming that the former is statistically representative of the actual cascade rate). This is because signed cascade rates require very large statistical samples to converge [10,26], which are not available to us for this Letter. However, by applying a linear fit on the resulting

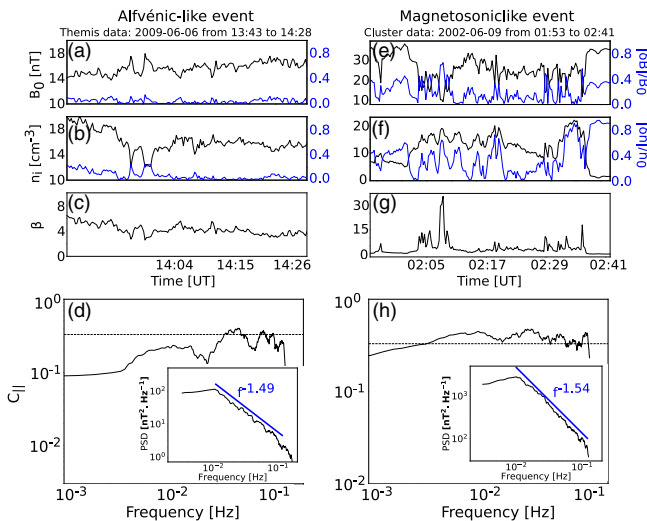


FIG. 1. (a), (e) The magnetic field modulus (black) and fluctuations (blue), (b), (f) ion number density (black) and density fluctuations (blue), and (c), (g) total plasma β . (d) and (h) the corresponding magnetic compressibility. The inset is the PSD of δB and the corresponding power-law fit in the inertial range (blue).

energy cascade rates, we considered only the ones that are relatively linear with τ and showed no sign change at least over one decade of scales in the inertial range. Two main observations can be made from the two examples shown in Fig. 2: first, the incompressible cascade rate $|\epsilon_I|$ is larger by a factor ~ 100 in the magnetosonic case compared to the Alfvénic one, which can be explained by the large amplitude δB in the former [10]. Second, density fluctuations in the magnetosonic case amplify $|\epsilon_C|$ by a factor ~ 7 with respect to $|\epsilon_I|$. The results of analysis of all the samples are summarized in Fig. 3. As one can see in that figure, for the incompressible Alfvénic cases, the histograms of $\langle |\epsilon_C| \rangle$ (blue) and $\langle |\epsilon_I| \rangle$ (red), almost overlap and the mean values for both are of the order of $\sim 10^{-14} \text{ J m}^{-3} \text{ s}^{-1}$, whereas for the compressible magnetosonic events the histogram of $\langle |\epsilon_C| \rangle$ (blue) is shifted towards larger values compared to $\langle |\epsilon_I| \rangle$ (red). The corresponding mean values are, respectively, $\sim 6 \times 10^{-13}$ and $\sim 2 \times 10^{-13} \text{ J m}^{-3} \text{ s}^{-1}$. We note that these values are dominated by the few samples that have the highest values of $\langle |\epsilon| \rangle$ (Fig. 4).

Interestingly, the role of the compressibility in increasing the compressible cascade rate can be evidenced by the turbulent Mach number $\mathcal{M}_s = \sqrt{\langle \delta v \rangle^2 / c_s^2}$, where δv is the fluctuating flow velocity. Figure 4 shows a power law-like dependence of $\langle |\epsilon_C| \rangle$ on \mathcal{M}_s as $\langle |\epsilon_C| \rangle \sim \mathcal{M}_s^4$, steeper than the one observed in the solar wind [10]. To the best of our knowledge, there are no theoretical predictions that relate ϵ to \mathcal{M}_s in compressible turbulence. However, in incompressible flows, dimensional analysis *à la* Kolmogorov yields a scaling that relates ϵ_I to the third power of \mathcal{M}_s . The high level of the density fluctuations in the magnetosheath seems to modify this scaling to the one we estimated here. Although more analytical and numerical studies are needed to understand the relationship between $|\epsilon_C|$ and \mathcal{M}_s , the scaling law obtained here may be used as an empirical model for other compressible media not accessible to *in situ* measurements.

A good correlation is also evidenced between the leading order of compressible internal energy $U = \rho_0 c_s^2 \ln(1 + \rho_1 / \rho_0)$ of the turbulent fluctuations and the cascade rate in the magnetosoniclike events. Figure 5 shows, for each type of turbulent fluctuation, the dependence of

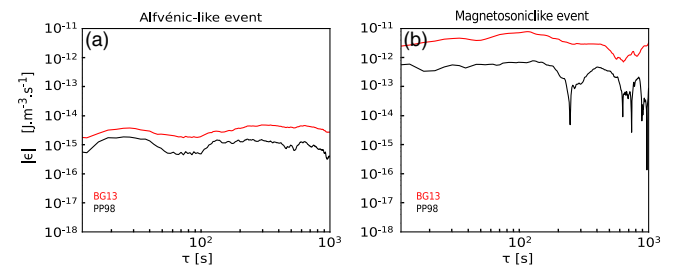


FIG. 2. The energy cascade rates computed using BG13 (red) and PP98 (black) for the same (a) Alfvénic and (b) magnetosoniclike events of Fig. 1.

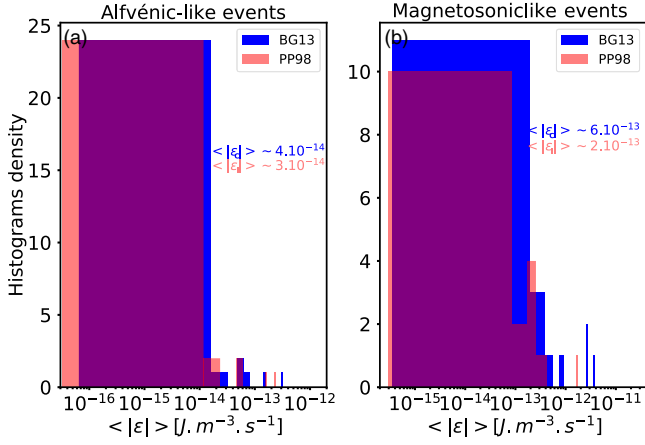


FIG. 3. Histograms of $\langle |\epsilon_I| \rangle$ (red) and $\langle |\epsilon_C| \rangle$ (blue) computed using the PP98 and BG13 exact laws for the (a) Alfvénic and (b) magnetosoniclike events.

$\langle |\epsilon_C| \rangle$ on the normalized (to U) kinetic energy $E_K = \frac{1}{2}\rho_0\delta v^2$ and magnetic energy $E_B = (1/2\mu_0)\delta B^2$, where δB and δv are, respectively, the fluctuating magnetic and flow velocity fields. First, one can see that, for both types of turbulence, E_B/U (blue) dominates over E_K/U (red). Moreover, for the magnetosoniclike cases, there is a general trend indicating that high $\langle |\epsilon_C| \rangle$ corresponds to increasing compressible internal energy which becomes comparable (or slightly larger) than the kinetic and magnetic energies at the highest values of $\langle |\epsilon_C| \rangle$. This trend is not seen on the Alfvénic cases indicating the prominent role of the internal energy in controlling the cascade rate. This last result contrasts significantly with the finding in the solar wind [10].

To study the anisotropic nature of the cascade rate for the different types of the MHD fluctuations, we examine the dependence of the estimated cascade rates on the mean angle $\Theta_{\mathbf{VB}}$ between the local magnetic and flow vectors. This approach has already been used in similar studies of

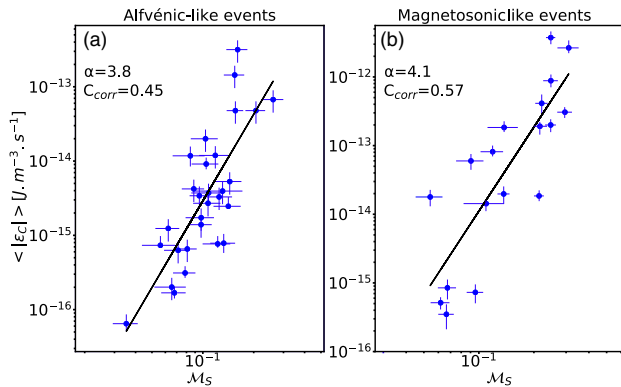


FIG. 4. Compressible energy cascade rate as a function of the turbulent Mach number for the Alfvénic (a) and magnetosoniclike (b) events. The black line represents a least square fit of the data, α is the slope of the power-law fit. The error bars represent the standard deviation of $|\epsilon_C|$.

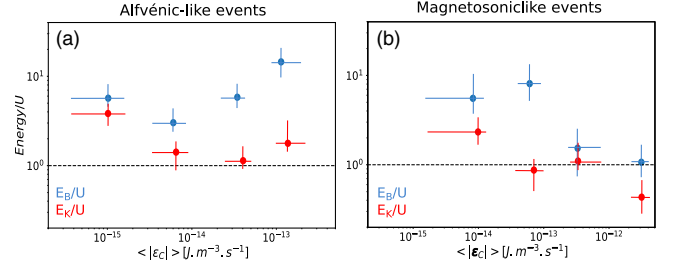


FIG. 5. Normalized mean compressible magnetic (blue) and kinetic (red) binned energies to the internal energy as a function of the binned compressible energy cascade rate for the Alfvénic (a) and magnetosonic (b) events.

solar wind turbulence [10,53,54]. Here, we consider only the events that have a relatively uniform $\Theta_{\mathbf{VB}}$ to guarantee that the spacecraft is sampling nearly the same direction of space for each time interval (using the Taylor frozen-in flow assumption). As one can see in Fig. 6, for both models, the cascade rate is lower in the parallel direction than in the perpendicular one. The same trend is observed for the total energy, except that, for the magnetosonic events, the highest cascade rate and total energy are observed at oblique angles $\Theta_{\mathbf{VB}} \sim 50^\circ - 60^\circ$ (see discussion below). The second important observation is that the density fluctuations seem to reinforce the anisotropy of the cascade rate with respect to the Alfvénic turbulence: The ratio $\mathcal{R} = \langle |\epsilon_C| \rangle / \langle |\epsilon_I| \rangle$ (in blue) is close to 1 for the Alfvénic cases, but increases to ~ 3 for the magnetosonic ones at quasi-perpendicular angles. Numerical simulations of compressible MHD turbulence showed that fast magnetosonic turbulence is spatially isotropic while slow mode turbulence is anisotropic and has a spectrum $k_\perp^{-5/3}$ similar to Alfvénic turbulence [13]. This first observation that density fluctuations enhance the anisotropy of the cascade rate suggests that a slowlike (or mirror) mode turbulence dominates the compressible fluctuations analyzed here [43,49]. This result agrees with the analysis of the stability conditions of the plasma derived from the linear Maxwell-Vlasov theory. Figure 7 shows that a large fraction of lowest values of the compressible cascade rate correspond

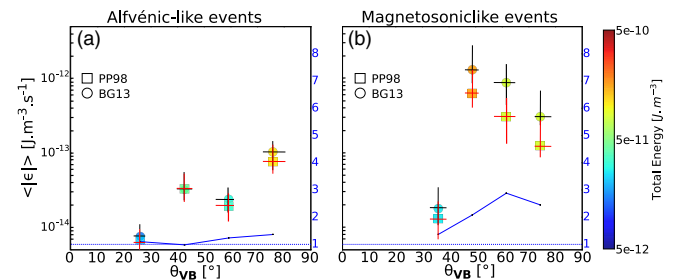


FIG. 6. Compressible and incompressible energy cascade rates $\langle |\epsilon_C| \rangle$ and $\langle |\epsilon_I| \rangle$ as a function of the mean angle $\Theta_{\mathbf{VB}}$ and the total energy (colored bar) for the Alfvénic (a) and magnetosonic (b) events. The blue line is the ratio $\mathcal{R} = \langle |\epsilon_C| \rangle / \langle |\epsilon_I| \rangle$.

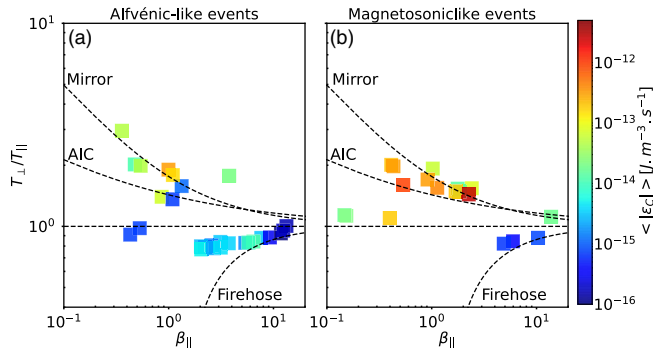


FIG. 7. Compressible energy cascade rate $\langle |e_C| \rangle$ averaged into bins of proton temperature anisotropy (T_{\perp}/T_{\parallel}) vs β_{\parallel} for (a) the Alfvénic and (b) magnetosoniclike events. The dashed lines correspond to the mirror, the Alfvénic ion cyclotron (AIC), and fire hose linear instabilities thresholds.

to Alfvénic-like events and lie close to the stability condition $T_{\perp}/T_{\parallel} \sim 1$. In contrast, most of the highest $\langle |e_C| \rangle$ correspond to magnetosonic events and lie near the mirror instability threshold. Considering that the maximum growth rate of the linear mirror instability occurs at oblique angles $\Theta_{\mathbf{kB}}$ (approximated here by the angle $\Theta_{\mathbf{VB}}$) [55], the peak of the cascade rate and the total energy observed for $\Theta_{\mathbf{VB}} \sim 50^{\circ}$ – 60° in Fig. 6 may be explained by energy injection into the background turbulent plasma through the mirror instability, which seems to enhance the dissipation rate. A similar relationship between the incompressible cascade rate and kinetic plasma instabilities was found in the solar wind [56], however, deeper understanding of the connection between these two features of plasma turbulence requires further theoretical investigation [57]. Although the Taylor hypothesis (implicitly used in this Letter to interpret time lags τ as spatial increments) cannot generally be tested in single spacecraft data, the dominance of anisotropic slowlike (or mirrorlike) modes and the intrinsic anisotropic nature of the Alfvénic turbulence are arguments in favor of the validity of the Taylor hypothesis [58]. Indeed, k -filtering results obtained from four samples of Cluster data intervals to which the technique could be applied, support this conclusion (see Supplemental Material [48]).

Conclusions.—The energy cascade rate in MHD turbulence in a the compressible magnetosheath plasma was found to be at least 2 orders of magnitude higher than in the (nearly) incompressible solar wind. Empirical laws relating the cascade rate to the turbulent Mach number were obtained. Density fluctuations were shown to amplify magnitude and the spatial anisotropy of the cascade rate in comparison to incompressible Alfvénic turbulence. This result and the analysis of the plasma stability conditions in the plane $(T_{\perp}/T_{\parallel}, \beta_{\parallel})$ indicate that the density fluctuations are carried by mirrorlike (slow magnetosoniclike) mode driven by proton temperature anisotropy. These new

fundamental features of compressible turbulence may have potential applications in the magnetosheath (e.g., turbulence-driven reconnection at the magnetopause [59,60]) and in distant astrophysical plasmas. For instance, recently, Zank *et al.* [15] showed the importance of the compressible magnetosonic modes in forming the turbulent energy cascade in the local ISM, the heliosheath (also a bounded region, by the termination shock and the heliopause) using *in situ Voyager 1* data, results similar to the ones reported here.

Helpful discussions with N. Andres, S. Banerjee, and H. Breuillard are gratefully acknowledged. The fields and the particles data of *Cluster* spacecraft come from the CAA (ESA) and of *THEMIS B/C* spacecraft from the AMDA science analysis system provided by the Centre de Données de la Physique des Plasmas (IRAP, Université Paul Sabatier, Toulouse) supported by CNRS and CNES (CDPP, IRAP, France). The French participation in *Cluster* and *THEMIS* are supported by CNES. L. Z. H., F. S. and S. G. acknowledge financial support from the ANR project THESOW, Grant No. ANR-11-JS56-0008 and from “Programme National Soleil-Terre (PNST)”.

*Corresponding author.

lina.hadid@irfu.se

- [1] Zimbaro, Magnetic turbulence in space plasmas: in and around the Earth’s magnetosphere, *Plasma Phys. Controlled Fusion* **48**, B295 (2006).
- [2] A. A. Schekochihin, S. C. Cowley, W. Dorland, G. W. Hammett, G. G. Howes, E. Quataert, and T. Tatsuno, Astrophysical gyrokinetics: Kinetic and fluid turbulent cascades in magnetized weakly collisional plasmas, *Astrophys. J. Suppl. Ser.* **182**, 310 (2009).
- [3] M. von Papen, J. Saur, and O. Alexandrova, Turbulent magnetic field fluctuations in Saturn’s magnetosphere, *J. Geophys. Res.* **119**, 2797 (2014).
- [4] C. Tao, F. Sahraoui, D. Fontaine, J. de Patoul, T. Chust, S. Kasahara, and A. Retino, Properties of Jupiter’s magnetospheric turbulence observed by the Galileo spacecraft, *J. Geophys. Res.* **120**, 2477 (2015).
- [5] P. Song, C. T. Russell, and M. F. Thomsen, Slow mode transition in the frontside magnetosheath, *J. Geophys. Res.* **97**, 8295 (1992).
- [6] F. Sahraoui, J. L. Pinçon, G. Belmont, L. Rezeau, N. Cornilleau-Wehrin, P. Robert, L. Mellul, J. M. Bosqued, A. Balogh, P. Canu, and G. Chanteur, ULF wave identification in the magnetosheath: The k -filtering technique applied to Cluster II data, *J. Geophys. Res.* **108**, 1335 (2003).
- [7] E. A. Lucek, D. Constantinescu, M. L. Goldstein, J. Pickett, J. L. Pincon, F. Sahraoui, R. A. Treumann, and S. N. Walker, The magnetosheath, *Space Sci. Rev.* **118**, 95 (2005).
- [8] V. Génot, E. Budnik, C. Jacquey, I. Dandouras, and E. Lucek, Mirror modes observed with Cluster in the Earth’s magnetosheath: Statistical study and IMF solar wind dependence, *Adv. Geosci.* **14**, 263 (2009).

- [9] G. G. Howes, S. D. Bale, K. G. Klein, C. H. K. Chen, C. S. Salem, and J. M. TenBarge, The slow-mode nature of compressible wave power in solar wind turbulence, *Astrophys. J. Lett.* **753**, L19 (2012).
- [10] L. Z. Hadid, F. Sahraoui, and S. Galtier, Energy cascade rate in compressible fast and slow solar wind turbulence, *Astrophys. J.* **838**, 9 (2017).
- [11] E. Vázquez-Semadeni, T. Passot, and A. Pouquet, Influence of cooling-induced compressibility on the structure of turbulent flows and gravitational collapse, *Astrophys. J.* **473**, 881 (1996).
- [12] Y. Lithwick and P. Goldreich, Compressible magnetohydrodynamic turbulence in interstellar plasmas, *Astrophys. J.* **562**, 279 (2001).
- [13] J. Cho and A. Lazarian, Compressible Sub-Alfvénic MHD Turbulence in Low- β Plasmas, *Phys. Rev. Lett.* **88**, 245001 (2002).
- [14] C. Federrath, J. Roman-Duval, R. S. Klessen, W. Schmidt, and M. M. Mac Low, Comparing the statistics of interstellar turbulence in simulations and observations. Solenoidal versus compressive turbulence forcing, *Astron. Astrophys.* **512**, A81 (2010).
- [15] G. P. Zank, S. Du, and P. Hunana, The origin of compressible magnetic turbulence in the very local interstellar medium, *Astrophys. J.* **842**, 114 (2017).
- [16] C.-Y. Tu and E. Marsch, MHD structures, waves and turbulence in the solar wind: Observations and theories, *Space Sci. Rev.* **73**, 1 (1995).
- [17] R. Bruno and V. Carbone, The solar wind as a turbulence laboratory, *Living Rev. Solar Phys.* **2**, 4 (2005).
- [18] F. Sahraoui, M. L. Goldstein, P. Robert, and Y. V. Khotyaintsev, Evidence of a Cascade and Dissipation of Solar-Wind Turbulence at the Electron Gyroscale, *Phys. Rev. Lett.* **102**, 231102 (2009).
- [19] H. Politano and A. Pouquet, von Kármán–Howarth equation for magnetohydrodynamics and its consequences on third-order longitudinal structure and correlation functions, *Phys. Rev. E* **57**, R21 (1998).
- [20] C. W. Smith, K. Hamilton, B. J. Vasquez, and R. J. Leamon, Dependence of the dissipation range spectrum of interplanetary magnetic fluctuations on the rate of energy cascade, *Astrophys. J. Lett.* **645**, L85 (2006).
- [21] L. Sorriso-Valvo, R. Marino, V. Carbone, A. Noullez, F. Lepreti, P. Veltri, R. Bruno, B. Bavassano, and E. Pietropaolo, Observation of Inertial Energy Cascade in Interplanetary Space Plasma, *Phys. Rev. Lett.* **99**, 115001 (2007).
- [22] B. Vasquez, C. W. Smith, K. Hamilton, B. T. MacBride, and R. J. Leamon, Evaluation of the turbulent energy cascade rates from the upper inertial range in the solar wind at 1 AU, *J. Geophys. Res.* **112**, A07101 (2007).
- [23] B. MacBride, C. W. Smith, and M. A. Forman, The turbulent cascade at 1 AU: Energy transfer and the third-order scaling for MHD, *Astrophys. J.* **679**, 1644 (2008).
- [24] J. E. Stawarz, C. W. Smith, J. Vasquez, M. A. Forman, and B. T. MacBride, The turbulent cascade and proton heating in the solar wind at 1 AU, *Astrophys. J.* **697**, 1119 (2009).
- [25] J. T. Coburn, C. W. Smith, B. J. Vasquez, J. E. Stawarz, and M. A. Forman, The turbulent cascade and proton heating in the solar wind during solar minimum, *Astrophys. J.* **754**, 93 (2012).
- [26] J. T. Coburn, M. A. Forman, C. W. Smith, B. J. Vasquez, and J. E. Stawarz, Third-moment descriptions of the interplanetary turbulent cascade, intermittency and back transfer, *Phil. Trans. R. Soc. A* **373**, 20140150 (2015).
- [27] J. W. Freeman, Estimates of solar wind heating inside 0.3 AU, *Geophys. Res. Lett.* **15**, 88 (1988).
- [28] E. Marsch, K. H. Muhlhauser, R. Schwenn, H. Rosenbauer, W. Pilipp, and F. M. Neubauer, Solar wind protons: Three-dimensional velocity distributions and derived plasma parameters measured between 0.3 and 1 AU, *J. Geophys. Res.* **87**, 52 (1982).
- [29] P. R. Gazis, Observations of plasma bulk parameters and the energy balance of the solar wind between 1 and 10 AU, *J. Geophys. Res.* **89**, 775 (1984).
- [30] P. R. Gazis, Solar wind velocity and temperature in the outer heliosphere, *J. Geophys. Res.* **99**, 6561 (1994).
- [31] J. D. Richardson, K. I. Paularena, A. J. Lazarus, and J. W. Belcher, Radial evolution of the solar wind from IMP 8 to Voyager 2, *Geophys. Res. Lett.* **22**, 325 (1995).
- [32] S. Banerjee and S. Galtier, Exact relation with two-point correlation functions and phenomenological approach for compressible magnetohydrodynamic turbulence, *Phys. Rev. E* **87**, 013019 (2013).
- [33] S. Banerjee, L. Z. Hadid, F. Sahraoui, and S. Galtier, Scaling of Compressible Magnetohydrodynamic Turbulence in the Fast Solar Wind, *Astrophys. J. Lett.* **829**, L27 (2016).
- [34] C. P. Escoubet, R. Schmidt, and M. L. Goldstein, Cluster–Science and mission overview, *Space Sci. Rev.* **79**, 11 (1997).
- [35] V. Angelopoulos, The THEMIS mission, *Space Sci. Rev.* **141**, 5 (2008).
- [36] A. Balogh, S. W. H. Cowley, M. W. Dunlop, D. J. Southwood, J. G. Thomlinson, K. H. Glassmeier, G. Musmann, H. Luehr, M. H. Acuna, and D. H. Fairfield, The Cluster magnetic field investigation: Scientific objectives and instrumentation, *Cluster: Mission, Payload, and Supporting Activities* (European space Agency, Paris, France, 1993).
- [37] H. Reme *et al.*, The cluster ion spectrometry (CIS) experiment, *Space Sci. Rev.* **79**, 303 (1997).
- [38] A. D. Johnstone, C. Alsop, S. Burge, P. J. Carter, A. J. Coates, A. J. Coker, A. N. Fazakerley, M. Grande, R. A. Gowen, C. Gurgiolo, B. K. Hancock, B. Narheim, A. Preece, P. H. Sheather, J. D. Winningham, and R. D. Woodliffe, Peace: A plasma electron and current experiment, *Space Sci. Rev.* **79**, 351 (1997).
- [39] J. G. Trotignon, P. M. E. Décréau, J. L. Rauch, E. Le Guirriec, P. Canu, and F. Darrouzet, The Whisper Relaxation Sounder Onboard Cluster: A Powerful Tool for Space Plasma Diagnosis around the Earth, *Cosmic Res. (Transl. of Kosm. Issled.)* **41**, 345 (2003).
- [40] H. U. Auster *et al.*, The THEMIS fluxgate magnetometer, *Space Sci. Rev.* **141**, 235 (2008).
- [41] J. P. McFadden, C. W. Carlson, D. Larson *et al.*, The THEMIS ESA plasma instrument and in-flight calibration, *Space Sci. Rev.* **141**, 277 (2008).
- [42] S. Y. Huang, L. Z. Hadid, F. Sahraoui, Z. G. Yuan, and X. H. Deng, On the existence of the kolmogorov inertial range in the terrestrial magnetosheath turbulence, *Astrophys. J. Lett.* **836**, L10 (2017).

- [43] L. Z. Hadid, F. Sahraoui, K. H. Kiyani, A. Retino, R. Modolo, P. Canu, A. Masters, and M. K. Dougherty, Nature of the MHD and kinetic scale turbulence in the magnetosheath of Saturn: Cassini observations, *Astrophys. J. Lett.* **813**, L29 (2015).
- [44] S. P. Gary and C. W. Smith, Short-wavelength turbulence in the solar wind: Linear theory of whistler and kinetic Alfvén fluctuations, *J. Geophys. Res.* **114**, A12105 (2009).
- [45] F. Sahraoui, G. Belmont, and M. L. Goldstein, New insight into short-wavelength solar wind fluctuations from Vlasov theory, *Astrophys. J.* **748**, 100 (2012).
- [46] C. S. Salem, G. G. Howes, D. Sundkvist, S. D. Bale, C. C. Chaston, C. H. K. Chen, and F. S. Mozer, Identification of kinetic Alfvén wave turbulence in the solar wind, *Astrophys. J. Lett.* **745**, L9 (2012).
- [47] T. Dudok De Wit, Can high-order moments be meaningfully estimated from experimental turbulence measurements?, *Phys. Rev. E* **70**, 055302 (2004).
- [48] See Supplemental Material at <http://link.aps.org/supplemental/10.1103/PhysRevLett.120.055102> for compressible magnetohydrodynamic turbulence in the Earth's magnetosheath: estimation of the energy cascade rate using in situ spacecraft data, which includes Refs. [49–52].
- [49] F. Sahraoui, G. Belmont, L. Rezeau, N. Cornilleau-Wehrin, J. L. Pincon, and A. Balogh, Anisotropic Turbulent Spectra in the Terrestrial Magnetosheath as Seen by the Cluster Spacecraft, *Phys. Rev. Lett.* **96**, 075002 (2006).
- [50] A. Mangeney, C. Lacombe, M. Maksimovic, A. A. Samsonov, N. Cornilleau-Wehrin, C. C. Harvey, J.-M. Bosqued, and P. Travnicek, Cluster observations in the magnetosheath; part I: anisotropies of the wave vector distribution of the turbulence at electron scales, *Ann. Geophys.* **24**, 3507 (2006).
- [51] F. Sahraoui, M. L. Goldstein, G. Belmont, P. Canu, and L. Rezeau, Three Dimensional Anisotropic k Spectra of Turbulence at Subproton Scales in the Solar Wind, *Phys. Rev. Lett.* **105**, 131101 (2010).
- [52] O. Alexandrova, C. Lacombe, A. Mangeney, R. Grappin, and M. Maksimovic, Solar wind wind Turbulent spectrum at the plasma kinetic, *Astrophys. J.* **760**, 121 (2012).
- [53] R. Marino, L. Sorriso-Valvo, R. D'Amicis, V. Carbone, R. Bruno, and P. Veltri, On the occurrence of the third-order scaling in high latitude solar wind, *Astrophys. J.* **750**, 41 (2012).
- [54] C. W. Smith, J. E. Stawarz, B. J. Vasquez, M. A. Forman, and B. T. MacBride, Turbulent Cascade at 1 AU in High Cross-Helicity Flows, *Phys. Rev. Lett.* **103**, 201101 (2009).
- [55] O. A. Pokhotelov, O. G. Onishchenko, R. Z. Sagdeev, M. A. Balikhin, and L. Stenflo, Parametric interaction of kinetic Alfvén waves with convective cells, *J. Geophys. Res.* **109**, A3 (2004).
- [56] K. T. Osman, W. H. Matthaeus, K. H. Kiyani, B. Hnat, and S. C. Chapman, Proton Kinetic Effects and Turbulent Energy Cascade Rate in the Solar Wind, *Phys. Rev. Lett.* **111**, 201101 (2013).
- [57] M. W. Kunz, A. A. Schekochihin, and J. M. Stone, Firehose and Mirror Instabilities in a Collisionless Shearing Plasma, *Phys. Rev. Lett.* **112**, 205003 (2014).
- [58] G. G. Howes, K. G. Klein, and J. M. TenBarge, Validity of the Taylor hypothesis for linear kinetic waves in the weakly collisional solar wind, *Astrophys. J.* **789**, 106 (2014).
- [59] G. Belmont and L. Rezeau, Magnetopause reconnection induced by magnetosheath Hall-MHD fluctuations, *J. Geophys. Res.* **106**, 10751 (2001).
- [60] H. Karimabadi, V. Roytershteyn, H. X. Vu, Y. A. Omelchenko, J. Scudder, W. Daughton, A. Dimmock, K. Nykyri, M. Wan, D. Sibeck, M. Tatineni, A. Majumdar, B. Loring, and B. Geveci, The link between shocks, turbulence, and magnetic reconnection in collisionless plasmas, *Phys. Plasmas* **21**, 062308 (2014).